Frequency-agile non-coherent ultrasound radar for collection of micro-Doppler signatures

Alessio Balleri and Karl Woodbridge
Dept. of Electronic & Electrical Engineering
University College London
London, UK, WC1E 7JE
Email: {a.balleri, k.woodbridge}@ee.ucl.ac.uk

Kevin Chetty
UCL Centre for Security and Crime Science
University College London
London, UK, WC1E 7HN
Email: k.chetty@ucl.ac.uk

Abstract— **Classification of targets by micro-Doppler signatures has attracted a growing interest in recent years. The main bulk translation of a target and additional target motions, such as vibrations and rotations, generate Doppler modulations in the echo that contain unique target features and thus can be used to perform target recognition. Although, target classification by micro-Doppler signatures has been exploited in the RF regime for radar systems, the frequency spectrum is becoming increasingly congested and expensive to use, so that it is desirable to identify and exploit other types which have similar capabilities. In this paper a frequency-agile non-coherent ultrasound radar developed to gather micro-Doppler signatures is presented. This was used in an experimental trial to gather micro-Doppler signatures of personnel targets whilst undertaking various types of motion. Classification performance by these same micro-Doppler signatures is then assessed and results discussed.**

I. INTRODUCTION

Echo returns from targets undergoing bulk translations experience a shift in frequency due to the well known Doppler effect [1]. In addition to this, any additional dynamics, such as vibrations or rotations of physical parts that compose the target, induce further Doppler modulations around the main Doppler shift that take the name of micro-Doppler modulations. Micro-Doppler modulations, or micro-Doppler signatures, provide extra information about the target of interest and thus can be used to perform target classification [2]. Most of the work on micro-Doppler target classification has been done at RF frequencies [3] [4] [5] [6] [7] [8] [9]. However, transmissions in these spectral bands are becoming increasingly congested and expensive, and this has been a driver towards finding valid substitutes. On the other hand, the development of radar systems, and the tendency and the necessity to develop more intelligent radars is resulting in the need of additional information, from other type of sensors, to be fused with the information obtained directly by the radar itself [10]. In this paper it is investigated whether it is possible to gather micro-Doppler signatures from targets at ultrasound frequencies. Limited data is currently available on acoustic micro-Doppler signatures at ultrasound frequencies. In [11] a continuous-wave ultrasound radar that is capable to detect human gait signatures at 40 kHz is described.

Ultrasound frequencies are successfully used in the natural world. Echolocating bats use ultrasound calls to sense the surrounding. Typical calls cover the frequencies range between 20 kHz up to 200 kHz, depending on the species of the bat. The type of waveforms and the modulation of the echolocation call both change as a function of the environment and the type of foraging. Interestingly, it has been shown that some species of bats largely rely on Doppler information, including micro-Doppler information, to select insects during foraging [12] [13] [14]. If micro-Doppler signatures are successfully used by bats to feed on insects and bats still rely on this for their survival after million of years, it is likely that a well developed acoustic radar can play an important part too. In this paper we describe a frequency-agile non-coherent acoustic radar that has been deployed to gather micro-Doppler signatures of humans taking a various number of actions. Classification performance is assessed on the gathered data.

II. TECHNICAL SPECIFICATION OF THE ACOUSTIC RADAR

The transmission section of the acoustic radar is composed of a signal generator which is connected to an amplifier and a loudspeaker. The receiver is based on a high-specification off-the-shelf acoustic camera composed of an array of microphones and a DAQ recorder. The signal is generated by a NI-PXI 6733 card, plugged into a NI chassis, that is capable of transmitting any type of waveforms up to 250 kHz with a resolution of 16 bits. The output of the signal generator feeds the input of a S55 Ultrasound Advice amplifier capable of operating from 18 kHz to 300 kHz. The maximum output of the amplifier is 140 V. The amplifier features a monitor output which allow monitoring the amplified exit with a factor $\div 100$. The amplified signal goes to a S56 Ultrasound Advice loudspeaker (50 mm active area diameter) capable of transmitting up to 300 kHz with SPL (Sound Pressure Level) of $>+105$dB in the range between 20 kHz and 50 kHz and $>+85$dB up to 150 kHz (at 0.25 m). The acoustic camera is composed of a set of arrays of microphones (two ring arrays, one spherical array, one star array) and a signal recorder. The recorder is capable of sampling echoes up to 194 kHz and therefore can be used with waveforms up to about 95 kHz. Each array of microphones is deployed with a video camera at its centre so that video data are recorded simultaneously with the acoustic data with the same time reference. This is quite useful in terms of micro-Doppler as it allows the

	Height	Arms	Hips	Shoulders
Target A	174 cm	67 cm	100 cm	46.5 cm
Target B	182 cm	69 cm	103.5 cm	45.5 cm

instantaneous motion of the target to be matched with the corresponding micro-Doppler signature. The acoustic camera is controlled by the $SimGen^{TM}$ software from which the operational parameters of the system are also defined. The radar is not coherent as transmitter and receiver do not use the same time references and because of this the exact time delay between transmission and reception is unknown at all times.

III. DESCRIPTION OF THE EXPERIMENT

The ultrasound radar was tested in an electromagnetic ane-choic chamber at UCL in April 2010. Although, not anechoic at ultrasound frequencies this proved to keep the level of noise low enough for our task and much lower than other available rooms. The 36-microphone ring array was placed next to the loudspeaker at about 1 m above the ground floor level. During this experiment only one microphone was utilised to record the echoes. Two personnel targets (*Target A* and *Target B*) facing the loudspeaker and the microphone at a distance of about 2.5 m were ensonified by a series of 4 sec single tones at 20 kHz and 40 kHz. Physical characteristics of the two targets are given in Table I. During the recording the two targets were swinging their arms whilst the position of the feet remained fixed at all times. No other restrictions were applied on the legs and the torso.

Fig. 1 shows the ultrasound micro-Doppler signature of *Target A* when a tone at 20 kHz was transmitted. This has been obtained by applying a Short Time Fourier Transform to the echo by using $T_w = 30$ msec long windows with a 50% overlap. The signature of the gait is clearly visible. The maximum frequency shift is about ± 900 Hz and occurs with a period of about 0.62 sec. The up-strokes (positive shifts) and down strokes (negative shifts) occur at almost the same time indicative of a special characteristic of this target's gait. Fig. 2 shows the results obtained from the same experiments on *Target B*. The signature of the gait is clearly visible with maximum shifts reaching about ± 1000 Hz. The period of the swing appears to be slightly shorter than that observed for *Target A* and equal to about 0.58 sec. Interestingly up-strokes and down-strokes do not occur simultaneously. This is well indicative of a different target gait. Fig. 3 and Fig. 4 show the results of the same experiment when a tone at 40 kHz was used to ensonify the targets. The signal to noise ratio is much lower in this case. This is partly due to the attenuation of the the ultrasound waves in air that at 40 kHz is higher (average of 0.5 dB/m higher depending on humidity) than that at 20 kHz. In addition to this, it became apparent that the return was
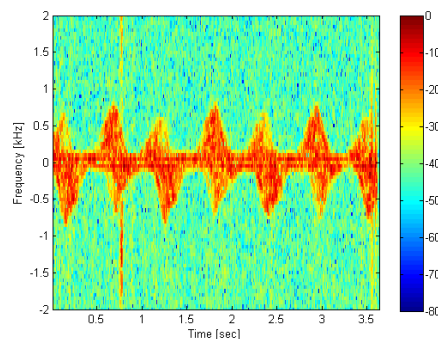

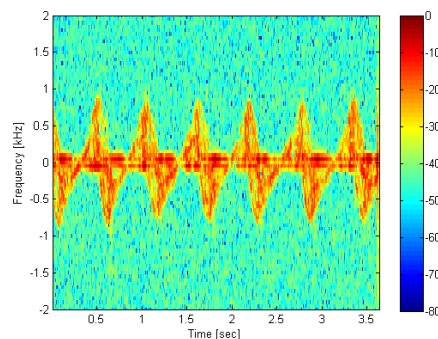Fig. 1. Micro-Doppler signature of *Target A* at 20 kHz.

Fig. 2. Micro-Doppler signature of *Target B* at 20 kHz.

also attenuated by a filter contained in the pre-amplifier of the acoustic camera that was designed to cut off the frequencies over 20-30 kHz. This is because the acoustic camera was firstly designed to be used in the audible acoustic range of frequencies for other applications, such as noise sound source localisation. Despite of this, the micro-Doppler signatures are still visible in both the images. The peaks are visible at higher frequencies over 1500 Hz (particularly in Fig. 4) and are swamped into noise at higher frequencies. The increase in the Doppler shift is in agreement with the mathematical expression for which the Doppler returns, equal to $f_D = f_0 V / c_s$, is directly proportional to the transmitted frequency f_0. In the formula, V is the radial velocity of the target with respect to the ultrasound radar and c_s is the speed of sound in air ($\simeq 343$ m/s). The periodicity of the gaits in the two images is in agreement with that observed at 20 kHz.

IV. CLASSIFICATION RESULTS

Classification performance was assessed on the data gathered at 20 kHz, i.e. those that presented the highest Signal to Noise Ratio. For each class, the received time sequence was divided in $Tw = 30$ msec long and 50% overlapping windows. The dimensionality of each window was reduced by extracting the first 15 MEL-Cepstrum coefficients [15]. These were calculated by filtering the Cepstrum of the each window, defined as

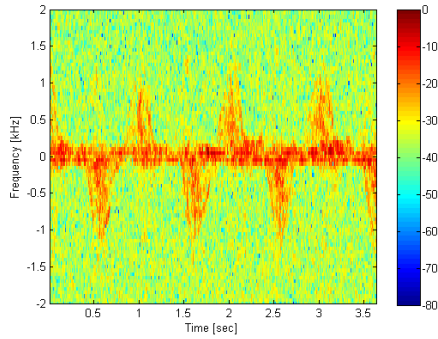$$C(k) = 10 * log10|X(k)| \qquad (1)$$

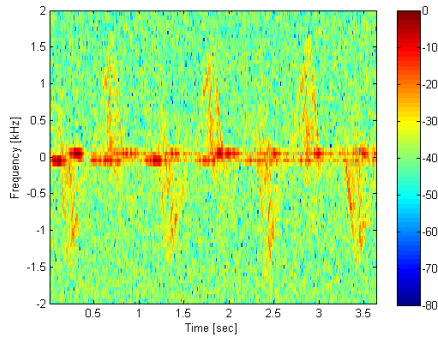Fig. 3.   Micro-Doppler signature of *Target A* at 40 kHz.

Fig. 4.   Micro-Doppler signature of *Target B* at 40 kHz.

with a bank of non-overlapping triangular filter, characterised by the same bandwidth $B = 300 \; mel$ and covering all the frequencies up to $F_s/2$. In the equation $X(k)$ corresponds to the DFT of the window $x(n)$ calculated at the digital frequency k. After dimensionality reduction the first $N = 100$ windows for each class were used to train a K-NN classifier set to make a decision using the $k = 3$ nearest neighbors to the classes. Classification performance was firstly tested on *Target A* and *Target B*. Fig. 5, that plots the first two MEL-Cepstrum features for each window in the 2D space, shows that after feature extraction the two classes are mainly overlapped. As expected, classification performance at the output of the classifier is poor and equal to 61%. The confusion matrix giving a detailed summary of all the decisions made by the classifier is given in Table II. Because of close similarities between the two micro-Doppler signatures the classifier shows a high rate of missed classification.

To investigate classification performance by micro-Doppler in the case of targets presenting different signatures *Target A* was then compared with a propeller that during the measurements was rotating at its highest speed and facing the array of microphones and the loudspeaker. The micro-Doppler signatures corresponding to the propeller was also obtained by calculating the Short Time Fourier Transform, with $T_w = 30$ msec long 50% overlapping windows, as for *Target A* and *Target B*. This is shown in Fig. 6. The corresponding plot of the first two MEL-Cepstrum coefficients
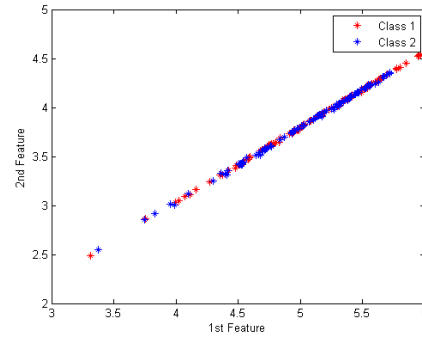

Fig. 5.   MEL-Cepstrum feature extraction. Feature 1 versus Feature 2 for *Target A* (blue) and *Target B* (red).

TABLE II

CONFUSION MATRIX FOR *Target A* AND *Target B*.

	Target A	*Target B*
Target A	83 (58.45%)	59 (41.55%)
Target B	51 (35.92%)	91 (64.08%)

is given in Fig. 7. In this case, after feature extraction the two classes are not completely overlapped and in particular, the features associated with the propeller present values that are higher than those associated with *Target A*. The probability of correct classification achieved by the K-NN classifier is now 94%. The confusion matrix giving all the decisions made by the classifier is given in Table III.

V. CONCLUSION

Results confirm that an acoustic radar can be used to detect micro-Doppler signatures at ultrasound frequencies. Although the radar can only survey limited ranges due to the high attenuation of sound in air, it could be deployed in indoor scenarios, such as airports, to monitor, for example, the flow of passengers and detect suspicious behavior. In addition to this, an ultrasound radar represents a simple and inexpensive tool which allows collection of micro-Doppler data that otherwise
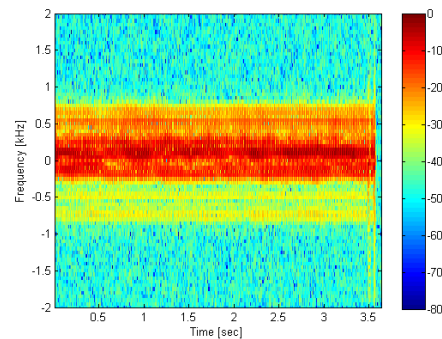

Fig. 6.   Micro-Doppler signature of a propeller, facing the array of microphones and the loudspeaker, ensonified with a 20 kHz constant pulse.
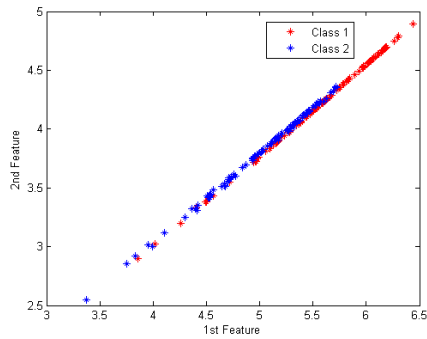
Fig. 7. MEL-Cepstrum feature extraction. Feature 1 versus Feature 2 for *Target A* (blue) and propeller (red).

TABLE III

CONFUSION MATRIX FOR *Target A* AND THE PROPELLER.

	Propeller	*Target A*
Propeller	137 (96.48%)	5 (3.52%)
Target A	11 (7.75%)	131 (92.25%)

would be difficult and expensive to obtain. This data could be used for the study of micro-Doppler signatures in a number of applications.

Future work will look at developing a coherent ultrasound radar capable of operating at higher frequencies for applications such as surveillance. In this application using the acoustic camera to record target return represents a fundamental limitation. Although the human hearing sensitivity is on the range of up to 20 kHz only, there are animals, such as cats and dogs, whose hearing system can detect frequencies up to 60 kHz. Because these are also likely to be ensonified in most applications, taking them into account becomes of great importance. Exploiting different waveforms that optimise the micro-Doppler return and improve classification of the data will also be at centre of our future work. This will be made possible by means of a new ultrasound microphone, capable of a higher sensitivity, that will be connected directly to the NI box allowing synchronisation between transmitter and receiver.

REFERENCES

[1] T. P. Gill, *The Doppler Effect, An Introduction to the Theory of the Effect.* Logos Press, Limited, 1965.
[2] V. Chen, F. Li, S.-S. Ho, and H. Wechsler, "Micro-doppler effect in radar: phenomenon, model, and simulation study," *IEEE Transactions on Aerospace and Electronic Systems*, vol. 42, no. 1, pp. 2–21, Jan. 2006.
[3] D. Tahmoush and J. Silvious, "Radar micro-doppler for long range front-view gait recognition," in *Biometrics: Theory, Applications, and Systems, 2009. BTAS '09. IEEE 3rd International Conference on*, 28-30 2009, pp. 1 –6.
[4] L. Vignaud, A. Ghaleb, J. Le Kernec, and J.-M. Nicolas, "Radar high resolution range & micro-doppler analysis of human motions," in *Radar Conference - Surveillance for a Safer World, 2009. RADAR. International*, 12-16 2009, pp. 1 –6.
[5] A. Ghaleb, L. Vignaud, and J. Nicolas, "Micro-doppler analysis of wheels and pedestrians in isar imaging," *Signal Processing, IET*, vol. 2, no. 3, pp. 301 –311, september 2008.
[6] G. Smith, K. Woodbridge, and C. Baker, "Naive bayesian radar micro-doppler recognition," in *Radar, 2008 International Conference on*, 2-5 2008, pp. 111 –116.
[7] G. E. Smith, K. Woodbridge, and C. J. Baker, "Template based micro-doppler signature classification," in *High Resolution Imaging and Target Classification, 2006. The Institution of Engineering and Technology Seminar on*, 21-21 2006, pp. 127 –144.
[8] G. Smith, K. Woodbridge, and C. Baker, "Micro-doppler signature classification," in *Radar, 2006. CIE '06. International Conference on*, 16-19 2006, pp. 1 –4.
[9] P. Sammartino and J. Fortuny-Guash, "Space and frequency diversity for moving personnel spectrogram estimation," *Conference proceedings on Radar 2010*, 2010.
[10] S. Haykin, "Cognitive radar: a way of the future," *IEEE Signal Processing Magazine*, vol. 23, no. 1, pp. 30 – 40, Jan. 2006.
[11] Z. Zhang, P. O. Pouliquen, A. Waxman, and A. G. Andreou, "Acoustic micro-Doppler radar for human gait imaging," *Journal of the Acoustical Society of America Express Letters*, vol. 121, no. 3, pp. 110–113, 2007.
[12] H.-U. Schnitzler, D. Menne, R. Kober, and K. Heblich, "The acoustical image of fluttering insects in echolocating bats," *Neuroethology and Behavioral Physiology*, pp. 235–250, 1983.
[13] H.-U. Schnitzler, "Echoes of fluttering insects: Information for echolocating bats," *Cambridge University Press*, pp. 226–243, 1987.
[14] R. C. Roverud, V. Nitsche, and G. Neuweiler, "Discrimination of wingbeat motion by bats, correlated with echolocation sound pattern," *Journal of Comparative Physiology A: Neuroethology, Sensory, Neural, and Behavioral Physiology*, vol. 168, pp. 259–263, 1991.
[15] S. Theodoridis and K. Koutroumbas, *Pattern Recognition - Fourth Edition*. Academic Press, 2009.